Research Article

Cancer Prevention Research

Dietary Tomato Powder Inhibits High-Fat Diet–Promoted Hepatocellular Carcinoma with Alteration of Gut Microbiota in Mice Lacking Carotenoid Cleavage Enzymes

Hui Xia[1], Chun Liu[1], Cheng-Chung Li[1], Maobin Fu[2], Shingo Takahashi[2], Kang-Quan Hu[1], Koichi Aizawa[1,2], Suganuma Hiroyuki[2], Guojun Wu[3], Liping Zhao[3], and Xiang-Dong Wang[1]

Abstract

Both incidence and death rate due to liver cancer have increased in the United States. Higher consumption of lycopene-rich tomato and tomato products is associated with a decreased risk of cancers. β-Carotene-15, 15′-oxygenase (BCO1), and β-carotene-9′, 10′-oxygenase (BCO2) cleave lycopene to produce bioactive apo-lycopenoids. Although BCO1/BCO2 polymorphisms affect human and animal lycopene levels, whether dietary tomato consumption can inhibit high-fat diet (HFD)–promoted hepatocellular carcinoma (HCC) development and affect gut microbiota in the absence of BCO1/BCO2 is unclear. BCO1/BCO2 double knockout mice were initiated with a hepatic carcinogen (diethylnitrosamine) at 2 weeks of age. At 6 weeks of age, the mice were randomly assigned to an HFD (60% of energy as fat) with or without tomato powder (TP) feeding for 24 weeks. Results showed that TP feeding significantly decreased HCC development (67%, 83%, and 95% reduction in incidence, multiplicity, and tumor volume, respectively, $P < 0.05$). Protective effects of TP feeding were associated with (1) decreased hepatic inflammatory foci development and mRNA expression of proinflammatory biomarkers (IL1β, IL6, IL12α, monocyte chemoattractant protein-1, and inducible NO synthase); (2) increased mRNA expression of deacetylase sirtuin 1 and nicotinamide phosphoribosyltransferase involving NAD^+ production; and (3) increased hepatic circadian clock genes (circadian locomotor output cycles kaput, period 2, and cryptochrome-2, Wee1). Furthermore, TP feeding increased gut microbial richness and diversity, and significantly decreased the relative abundance of the genus *Clostridium* and *Mucispirillum*, respectively. The present study demonstrates that dietary tomato feeding independent of carotenoid cleavage enzymes prevents HFD-induced inflammation with potential modulating gut microbiota and inhibits HFD-promoted HCC development. *Cancer Prev Res; 11(12); 797–810. ©2018 AACR.*

Introduction

Nonalcoholic fatty liver disease (NAFLD) affects 30%, 20%, and 3% to 10% of adult men, women, and children, respectively, in the United States. About 3% of NAFLD can progress to the inflammatory stage, nonalcoholic steatohepatitis (NASH), which can then progress to cirrhosis and liver failure, in which a liver transplant is a patient's only hope, and end-stage liver disease, such as primary liver cancer (hepatocellular carcinoma, HCC; refs. 1, 2). Recently, both incidence and death rate of liver cancer have increased in the United States (3). The future burden of liver cancer in 30 countries around 2030 has been predicted: the largest increases in rates are in the United States (4). The prevalence of NAFLD among the normal weight population and obese adults has been reported to be 25% and 67.5%, respectively, despite a higher risk factor of the obesogenic lifestyle for NAFLD (5). Furthermore, NAFLD can be related to alterations in gut microbiota dysbiosis, play a role in the development of a chronic low-grade inflammatory state

[1]Nutrition and Cancer Biology Laboratory, Jean Mayer USDA Human Nutrition Research Center on Aging at Tufts University, Boston, Massachusetts. [2]Nature and Wellness Research Department, Research and Development Division, Kagome Co., Ltd., Tochigi, Japan. [3]Department of Biochemistry and Microbiology, School of Environmental and Biological Sciences, Rutgers University, New Brunswick, New Jersey.

H. Xia, C. Liu, and C.-C. Li contributed equally to this article.

Corresponding Author: Xiang-Dong Wang, Jean Mayer United States Department of Agriculture Human Nutrition Research Center on Aging at Tufts University, 711 Washington St., Boston, MA 02111. Phone: 617-556-3130; Fax: 617-556-3344; E-mail: xiang-dong.wang@tufts.edu

doi: 10.1158/1940-6207.CAPR-18-0188

in the host (6), and promote progression of NASH (7) and HCC (8). HCC patients with NAFLD had a more advanced tumor stage and shorter survival time (9). Given the poor prognosis and high mortality rate of HCC, and no effective therapeutic agent that can halt the development and progression of HCC, it is important to discover a diet rich in effective chemopreventive agents against HCC development.

Epidemiologic studies suggest an inverse relationship between the consumption of lycopene-rich tomatoes and tomato products and plasma lycopene levels with the risk of cancer development (10, 11), although this association remains to be explored with liver cancer. Lycopene, one of the major carotenoids principally responsible for the characteristic deep-red color of ripe tomatoes and tomato products, has attracted attention due to its biological and physicochemical properties, especially related to its effects as a natural antioxidant (10, 12, 13). Experimental studies also provide evidence that lycopene may act as an anti-inflammatory/anticarcinogenic agent against certain types of diseases, including those of the liver, lung, colon, and prostate (11, 13). We have previously demonstrated that both lycopene and apo-10′-lycopenoic acid, a lycopene metabolite produced by β-carotene-9′, 10′-oxygenase (BCO2) cleavage, can significantly inhibit high-fat diet (HFD)–promoted HCC development in animals via different mechanisms in the absence of BCO2 (14, 15). Although BCO2 can catalyze lycopene into bioactive apo-10′-lycopeniods (16, 17), it was also shown that a central cleavage product apo-15′-lycopenal was detected when lycopene was incubated with human recombinant beta-carotene-15, 15′-oxygenase (BCO1) *in vitro* (18). Both BCO1 and BCO2 are highly expressed in the liver (19). These studies raised an important question of whether the protective effect of tomato and tomato products can be affected by these carotenoid cleavage enzymes (20). Previous studies have suggested that SNPs in the human *BCO1* gene are common and associated with reduced catalytic activity in the conversion of β-carotene to vitamin A (21, 22). The SNP of *BCO2* has been associated with alterations in the status of human and animal carotenoid levels, proinflammatory cytokine IL18 expression, and fasting high-density lipoprotein cholesterol levels (23–25). These observations suggest that the conflicting clinical trials' results, studying the role of carotenoid's chemopreventive effects, might be associated with the existence of BCO1/BCO2 polymorphism and their conversion of carotenoids into biological active metabolites in humans. Indeed, we observed that $BCO1^{-/-}/BCO2^{-/-}$ double knockout (KO) mice developed liver steatosis and had significantly higher levels of triglyceride in the liver and plasma compared with wild-type animals (26). Very recently, we found that dietary tomato powder (TP) feeding inhibited NAFLD in the $BCO1^{-/-}/BCO2^{-/-}$ double KO mice by upregulating sirtuin 1 (SIRT1) activity and AMP-activated protein kinase (AMPK) phosphorylation, decreasing lipogenesis and hepatic fatty acid uptake, and increasing fatty acid β-oxidation (27). However, (1) whether the whole tomato feeding can inhibit HFD-promoted inflammation and HCC development is unclear; (2) the importance of BCO1 and BCO2 in biological activities of the whole tomato against HCC development is unknown; and (3) the effects of the whole tomato feeding on gut microbiota in HFD-promoted hepatic tumorigenesis has not been explored. These notions clearly warrant evaluation.

In the present study, we investigated the effects of dietary TP feeding on the hepatic carcinogen (diethylnitrosamine, DEN)-initiated, HFD-promoted HCC development in the absence of BCO1 and BCO2 enzymes. In addition, we explored the influence of TP feeding on gut microbiome in this HFD-promoted hepatic tumorigenesis mouse model.

Materials and Methods

Study design

This study was approved by the Institutional Animal Care and Use Committee at the Jean Mayer USDA Human Nutrition Research Center on Aging (JM-HNRCA) at Tufts University. Male $BCO1^{-/-}BCO2^{-/-}$ double KO mice were previously generated as described (27, 28). Mice were bred in an Association for Assessment and Accreditation of Laboratory Animal Care–accredited animal facility at the JM-HNRCA at Tufts University. At 2 weeks of age, mice were injected i.p. with a liver-specific carcinogen, DEN (>99.9% purity, Sigma-Aldrich) with a dose of 25 mg/kg body weight. DEN was dissolved in normal saline with concentration at 2.5 mg DEN/mL. The infant mice were injected i.p. with 10 μL DEN/g body weight or sham saline at 2 weeks of age. At 6 weeks of age, mice were fed an HFD as a promoter for hepatic tumorigenesis with or without dietary TP intervention for 24 weeks: High fat diet [DEN+HFD group, $n = 9$, semipurified diet F3282, 60% calories from fat (C18:2 linoleic fatty acid, 36.6 gm/kg; C18:3 linolenic fatty acid, 3.6 gm/kg; total Saturated fatty acid, 141 gm/kg; total monounsaturated fatty acid, 162 gm/kg; total polyunsaturated fatty acid, 40.2 gm/kg); BioServ] or HFD with TP (DEN+HFD+TP group, $n = 9$, TP, 41.9 g/kg diet, Kagome, Inc.), as described (27). The specific batch of TP used in this study contained 2.39 mg of lycopene, 0.11 mg of β-carotene, 0.29 mg of ascorbic acid, and 0.32 mg of α-tocopherol per gram of TP, analyzed by high-performance liquid chromatography (HPLC). We did not determine all other nutrients for this specific batch of TP. The dose of TP was referred to the lycopene supplementation, which was found to inhibit HFD-induced fatty liver disease in our previous study (27) which indicated that the lycopene-supplemented dose of 100 mg/kg diet is equivalent to approximately 8.1 mg lycopene/day in a 60 kg adult man. According to the USDA

food composition database (USDA, 2012, Available from: http://ndb.nal.usda.gov/ndb/search/list), the average amount of lycopene is around 2.57 mg per 100 g in red tomato or 15 mg per 100 g in tomato sauce. In order to achieve the equivalent dose of 8.1 mg lycopene per day, one would need to consume approximately 3 medium-sized tomatoes (e.g., one medium tomato weighs approximately 125 g) or 1/4 cup of tomato sauce (1 cup = 245 g) per day. Mice were euthanized and sacrificed at 30 weeks of age. One mouse from the DEN+HFD group died for unknown reasons. The liver, visceral adipose tissues, and caecum fecal samples were harvested for further analysis.

Liver tumors' quantification

Whole livers were removed from mice after euthanization. Surface liver tumors (tumor multiplicity) were counted by two investigators blinded to treatments, and the tumor diameters were measured with a caliper to calculate tumor volume (volume $= 4/3\pi r^3$, where $r =$ diameter/2). Liver weights were recorded. Large surface tumors were removed, snap-frozen in liquid nitrogen, and stored at −80°C. The left lobe of mouse liver was fixed in 10% buffered formalin solution for further histopathologic analyses. The remaining sections of liver were divided into smaller portions, snap-frozen in liquid nitrogen, and stored at −80°C.

Histopathologic analyses

The left lobe of mouse liver was fixed in a 10% neutral buffered formalin solution (Thermo Fisher Scientific), followed by tissue processing, embedding, and sectioning. Five-micrometer sections of formalin-fixed and paraffin-embedded liver tissue were stained with hematoxylin and eosin (H&E, Sigma Aldrich) for histopathologic analysis. The sections were examined under light microscopy by two independent investigators who were blind to the treatment groups for HCC, hepatic steatosis, and hepatic inflammatory foci. Specifically, the liver tumor was confirmed as HCC according to the following histopathologic criteria as previously described (14): (1) the presence of trabecular pattern with 3+ cell-thick hepatocellular plates/cords; (2) mitotic figure; (3) enlarged convoluted nuclei or high nuclei/cytoplasmic ratio; (4) the presence of tumor giant cells with compact growth pattern; and (5) the presence of endothelial cells lining of sinusoids that surround enlarged hepatocellular plates/cords. Hepatic steatosis was graded according to steatosis magnitude (both macro- and microvesicular fat accumulation). Briefly, the degree of steatosis was graded based on the percentage of the liver section that was occupied by fat vacuoles at 100x magnification in 20 fields [grade 0 = < 5% (normal liver); grade 1 = 5%–25%; grade 2 = 26%–50%; grade 3 = 51%–75%; grade 4 = >75%]. Hepatic Inflammatory foci, characterized by clusters of recruited immune cells, were analyzed in 20 random fields at 100× magnification and represented as the number of foci per cm^2. A ZEISS microscope, equipped with a PixeLINK USB 2.0 (PL-B623CU) digital Camera and PixeLINK μScope Microscopy Software, was applied to quantify and capture images for all histopathologic analyses.

HPLC analysis

Lycopene concentrations in liver tissue were evaluated by HPLC techniques at 472 nm and quantified utilizing the area under the curve respective to an appropriate standard curve as previously described (27). Procedures were carried out under red light, and extraction efficiency was guaranteed by an internal control (echinenone).

RNA extraction and RT-PCR analysis

Liver tissues were used to extract total RNA with Trizol reagent (Roche Applied Science). A complementary DNA synthesis kit was used for reverse transcription of RNA. An ABI 7500 Real-Time PCR System (Applied Biosystems) equipped with a SYBR Green qPCR Mix (Roche Applied Science) was used to perform the analysis. The mRNA levels were calculated by the equation $2^{-\Delta\Delta CT}$ and presented as the fold change in gene expression normalized to the internal control, β-actin.

Protein extraction and Western blotting analysis

The following antibodies were used for Western blotting: primary antibodies for SIRT1, for both acetylated-fork head box protein O1 (FoxO1; Cell Signaling Technology), and total-FoxO1, phosphorylated- and total-AMPK (Cell Signaling Technology), nicotinamide phosphoribosyltransferase (NAMPT) from Sigma-Aldrich, and acetylated- and total NF-κB p65 (Cell Signaling Technology). Monoclonal mouse antibody against β-actin was purchased from Sigma-Aldrich. The secondary antibodies included horseradish peroxidase–conjugated anti-rabbit, anti-mouse antibodies (Bio-Rad). Protein extraction from liver tissues and Western blotting were performed as previously described (15). The relative intensity was measured to quantify protein levels using GS-710 Calibrated Imaging Densitometer (Bio-Rad). All blots were quantified and normalized against β-action to adjust for the amount of protein loaded.

Gut microbial 16s rRNA gene sequencing and analysis

Bacteria DNA was extracted from caecum samples at the end of the experiment using the QIAamp fast DNA Stool Mini Kit (Qiagen) according to the manufacturer's instructions. The V1-V2 region of 16S rDNA was amplified using Library quantification, and normalization and pooling were conducted according to the 27Fmod (5′-agrgtttgatymtggctcag-3′) and 338R (5′-tgctgcctcccgtaggagt-3′) as described (27, 29). The Nextera XT Index Kit was utilized to add Illumina sequencing adapters and multiplexing indices for further amplification. Sequencing was carried out using a paired-end, 2 × 300-bp cycle run on an Illumina MiSeq sequencing system (Illumina) and MiSeq

v3 reagent kits (600 Cycles, 15 Gb output), followed by a mixture of Pooled libraries denaturation and Illumina-generated PhiX control libraries by fresh NaOH. FastQ files were generated at the end of the run to perform quality control. The quality of the run was internally checked using PhiX Control, and then each pair-end sequence was assigned to corresponding samples according to the multiplexing indexes. Pair end reads were joined by command fastq-join contained in package ea-utils and then processed using a pipeline constructed as described (27). The raw paired end reads were assembled by pandaseq.

The reads were conducted with average quality scores of more than 25. After primer sequences were trimmed, 5,000 high-quality reads per sample were selected for the operational taxonomic unit (OTU) using a 97% pairwise-identity cutoff with the UCLUST program (27). Specific taxa of 16S OTUs and Alpha-diversity indices (ACE, Chao1, Shannon's index, and Simpson's index) were used to analyze the data with vegan (R package, v2.2-1).

Statistical analysis

SAS 9.3 software was used to assess normality and equal variance. GraphPad Prism 5 was used to perform all analyses. Student *t* tests and Mann–Whitney tests were used to examine the differences between DEN+HFD and DEN+HFD+TP groups. Data are expressed as mean and SEM or medians. A P value <0.05 was considered significant.

Results

TP feeding inhibited hepatic tumorigenesis in BCO1$^{-/-}$BCO2$^{-/-}$ double KO mice

TP feeding had no effect on body, liver, or visceral fat weight compared with the DEN+HFD group. TP feeding increased hepatic lycopene concentration with 5.0 ± 0.7 nmol/g (Table 1) which was within the range of lycopene concentrations in normal human liver (0.2–20.7 nmol/g tissue; ref. 30). DEN initiation with HFD feeding resulted in visible and multiple surface liver tumors in all of BCO1$^{-/-}$BCO2$^{-/-}$ double KO mice (Fig. 1A), which were confirmed by histopathologic examination according to the diagnostic criteria for HCC (Fig. 1B and C). The HCC (Fig. 1B and C, left) and normal liver tissue (Fig. 1B and C, right) were shown with H&E staining of ×100 and ×400 magnification under microscope, respectively. The incidence of HCC decreased by 67% after TP feeding (Table 1) compared with the mice fed an HFD alone. TP feeding significantly decreased the multiplicity (83%) and volume (95%) for HCC, as compared with the mice fed an HFD alone (Table 1).

Table 1. Body weight, liver weight, visceral fat weight, hepatic lycopene concentration, and tumor outcomes

	DEN+HFD	DEN+HFD+TP
Number of mice	$n = 8$	$n = 9$
Final body weight, g	55.6 ± 4.1	48.9 ± 4.2
Liver weight, g	2.6 ± 0.3	2.3 ± 0.4
Visceral fat weight, g	2.3 ± 0.2	2.2 ± 0.2
Hepatic lycopene (nmol/g liver)	ND	5.0 ± 0.7
Liver tumor incidence, %	100	33.3[a]
Multiplicity, #	9.8 ± 1.8	1.7 ± 0.8[a]
Volume, mm^3	1007.5 ± 449.6	25.4 ± 20.6[a]

NOTE: Student t test was used to examine the difference between DEN+HFD and DEN+HFD+TP.
Abbreviation: ND, not detected.
[a]P < 0.05 for comparison between DEN+HFD and DEN+HFD+TP.

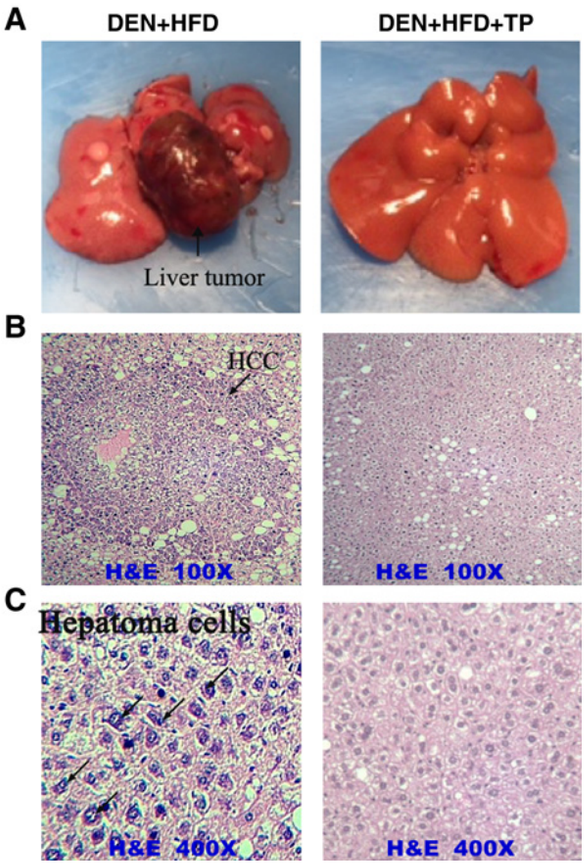

Figure 1.
Liver tumor quantification and histopathologic examination of liver tumor in BCO1$^{-/-}$BCO2$^{-/-}$ double KO mice fed with DEN+HFD or DEN+HFD+TP. **A,** The total liver organ was exhibited between DEN+HFD and DEN+HFD+TP groups. **B** and **C,** The histopathologic images of livers with H&E staining under 100x and 400x magnification of microscope, respectively.

TP feeding increased SIRT1 activity and NAMPT expression and modulated expression of circadian rhythm–related genes in BCO1$^{-/-}$BCO2$^{-/-}$ double KO mice

SIRT1 is an NAD-dependent protein deacetylase, catalyzing the deacetylation of many histones and nonhistone proteins including NF-κB, FOXOs (forkhead transcription factors), p53, etc., which has been implicated in the regulation of obesity-related inflammation and metabolic syndrome-associated cancer (31). TP feeding increased

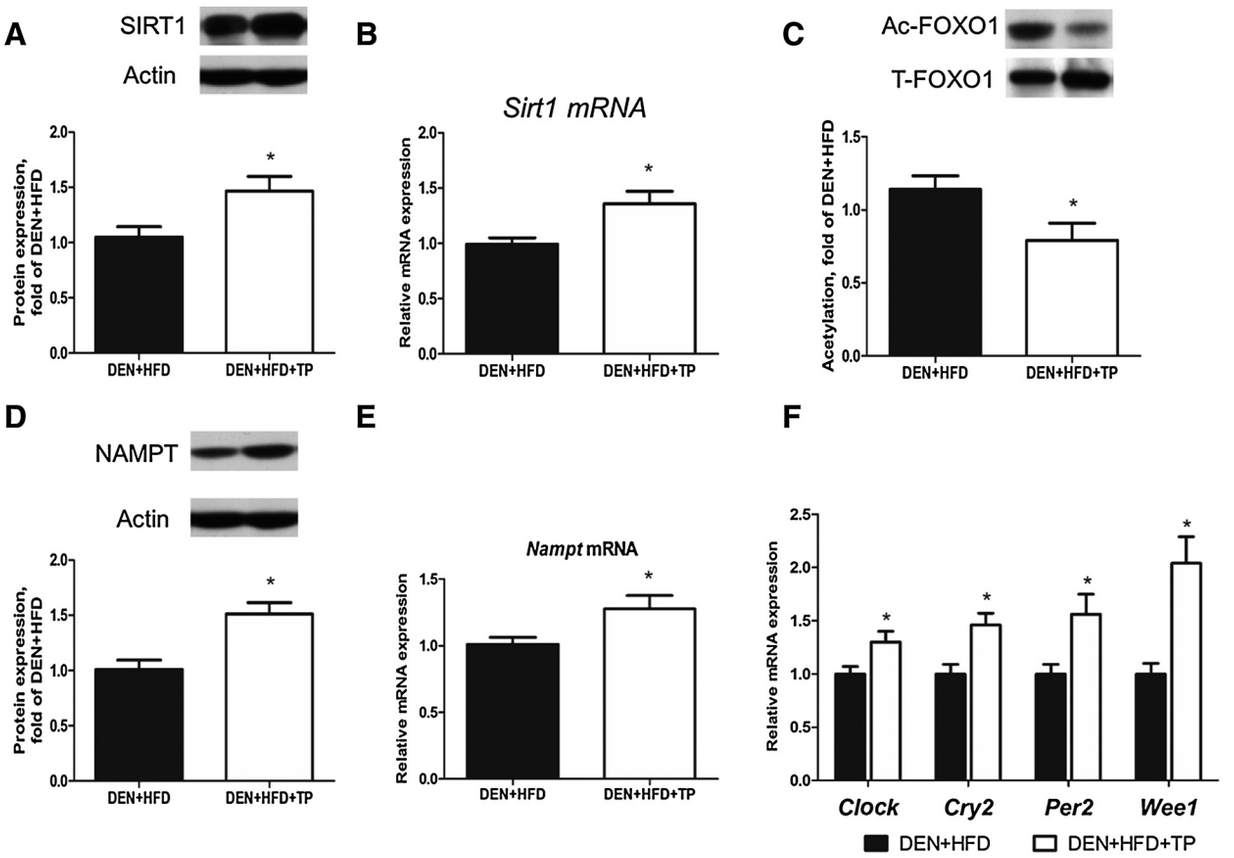

Figure 2.

Effects of TP feeding on hepatic mRNA and protein expression of SIRT1, SIRT1 activity, NAMPT, and hepatic mRNA expression of circadian clock–related genes in DEN+HFD-fed BCO1$^{-/-}$BCO2$^{-/-}$ double KO mice. Beta-actin was used as control unless specified otherwise. Graphical representation of fold change in (**A**) SIRT1 protein, (**B**) Ac-FOXO1 protein, (**C**) Sirt1 mRNA, (**D**) NAMPT protein, (**E**) NAMPT mRNA, and (**F**) Clock, Cry2, Per2, Wee1 mRNAs. Values are expressed as mean ± SEM. Differences between groups were analyzed by the Student *t* test. *Significantly different from the DEN+HFD, $P < 0.05$. Clock, circadian locomotor output cycles kaput; Cry2, cryptochrome-2; Per2, period 2.

both hepatic SIRT1 protein and mRNA levels significantly in BCO1$^{-/-}$BCO2$^{-/-}$ double KO mice, as compared with DEN+HFD mice (Fig. 2A and B). TP feeding significantly induced the deacetylation of SIRT1 direct targets and FOXO1 (e.g., reduction of acetylated FOXO1 in Fig. 2C). Because the rate-limiting enzyme, NAMPT, is one of the key target genes of BMAL and CLOCK to generate NAD^+ for SIRT1 deaceylase activity, we are interested in exploring whether the induction of SIRT1 activity by dietary TP restores circadian rhythmicity or expressions of distinct circadian clock genes, thereby increasing expression of NAMPT and preventing HFD-induced inflammation, metabolic alteration, and HFD-promoted HCC development. Results showed that TP feeding promoted the NAMPT protein and mRNA expression significantly compared with the DEN+HFD group (Fig. 2D and E). We also observed that mRNA expression of the circadian rhythm–related gene expression including Clock, Cry2, Per2, and Wee1 was more significantly upregulated in the DEN+HFD+TP group than in the DEN+HFD group in Fig. 2F, indicating potential regulating effects of TP on SIRT1/circadian clock/NAMPT axis in the liver of mice.

TP feeding ameliorated steatosis severity and modulated lipid metabolism in BCO1$^{-/-}$BCO2$^{-/-}$ double KO mice

The average steatosis score for the DEN+HFD+TP group was significantly lower than the DEN+HFD group in Fig. 3A and B, which suggest TP feeding suppressed the development of hepatic steatosis. Energy-consuming biosynthetic pathways were reported to be related to the phosphorylation and activation of AMPK, such as fatty acid and sterol synthesis (15). Phosphorylation and total AMPK protein levels increased near 50% compared with the DEN+HFD group (Fig. 3C). In addition, the downstream genes of AMPK were detected, and peroxisome proliferator-activated receptor-gamma coactivator-1α (PGC-1α), Acyl-CoA oxidase 1 (ACOX1), carnitine

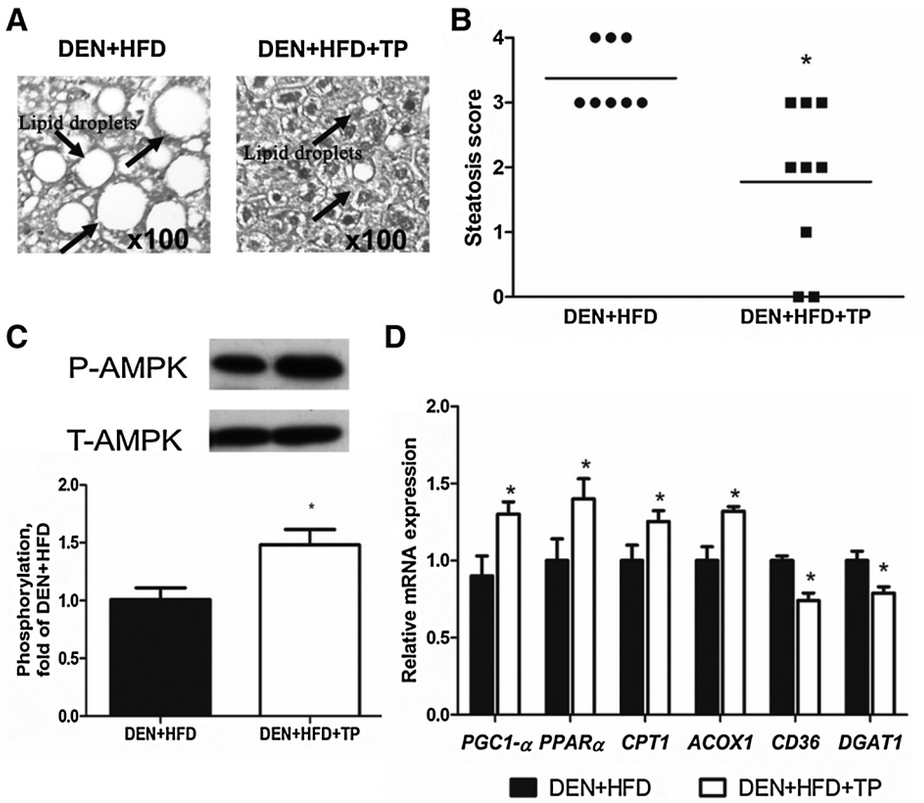

Figure 3.
Effects of TP feeding on steatosis severity and hepatic mRNA and protein expression of AMPK and its downstream gene mRNA expression in DEN+HFD-fed $BCO1^{-/-}BCO2^{-/-}$ double KO mice. The histopathology images of (**A**) hepatic steatosis and (**B**) hepatic steatosis score are presented. Graphical representation of fold change in (**C**) P-AMPK protein and (**D**) PGC-1, PPARα, CPT1, ACOX1, CD36, and DGAT1 genes. Values are expressed as mean ± SEM. Differences between groups were analyzed by Student *t* test. *Significantly different from the DEN+HFD, $P < 0.05$. PPARα, peroxisome proliferator-activated receptor α.

palmitoyltransferase 1 (CPT1), and peroxisome proliferator-activated receptor α (PPAR-α) mRNA levels in DEN+HFD+TP mice increased significantly compared with the DEN+HFD group in Fig. 3D. The expression levels of diacylglycerol acyltransferase 1 (DGAT1) and cluster of differentiation 36 (CD36) genes decreased more significantly in the TP feeding group than in the HFD control group.

TP feeding decreased the number of inflammatory foci and expression of proinflammatory-related genes in $BCO1^{-/-}BCO2^{-/-}$ double KO mice

In the present study, H&E staining of liver tissues showed the infiltration of inflammation foci cells in both DEN+HFD and DEN+HFD+TP groups (Fig. 4A). TP feeding reduced the number of hepatic inflammation foci (89%, $P < 0.05$) compared with the DEN+HFD group (Fig. 4B). TP feeding significantly reduced hepatic proinflammation biomarkers including NF-κB p65 acetylation (the deacetylation of SIRT1) and total protein expression (Fig. 4C), monocyte chemoattractant protein-1 (MCP1), inducible NO synthase (iNOS), TNFα, IL1β, IL6, and IL12α mRNA levels (Fig. 4D).

TP feeding changed the composition of gut microbiota in $BCO1^{-/-}BCO2^{-/-}$ double KO mice

To explore the profiling changes of the gut microbiota composition in mice after TP feeding, we performed 16S rDNA sequencing by the Illumina MiSeq platform. We detected a statistical difference in α-diversity at the observed OTUs ($P < 0.001$), CHAO1 ($P = 0.003$), and ACE ($P = 0.003$) diversity between both HFD+DEN+TP and HFD+DEN groups (Fig. 5A), which indicated that TP feeding increased the richness of intestinal microbiome. TP supplementation also increased microbial diversity significantly (Fig. 5B) using the Shannon–Weaver diversity index ($P = 0.02$).

The relative abundance of gram-positive bacteria exhibited an increased trend after TP feeding at the phylum level; meanwhile, the relative abundance of gram-negative bacteria decreased accordingly (Fig. 5C). Analysis at the phylum level indicated that the fecal microbiota was dominated by six major phyla: *Bacteroidetes*, *Firmicutes*, *Deferribacteres*, *Proteobacteria*, *Actiobacteria*, and *Tenericutes*. Among them, three major phyla (*Bacteroidetes*, *Firmicutes*, and *Deferribacteres*) were most predominant in fecal samples and comprised >96% in the HFD+DEN and HFD+DEN+TP groups (Fig. 5D). A lower proportion of relative abundance of *Bacteroidetes* ($P > 0.05$) and *Deferribacteres* ($P = 0.047$) was shown in the TP feeding group, compared with the HFD+DEN group. The TP feeding group showed a higher proportion trend for relative abundance of *Firmicutes*, compared with the DEN+HFD group. At the genus level, among 10 genera, *Bacteroides*, *Mucispirillum*, *Clostridium*, *Lactobacillus*,

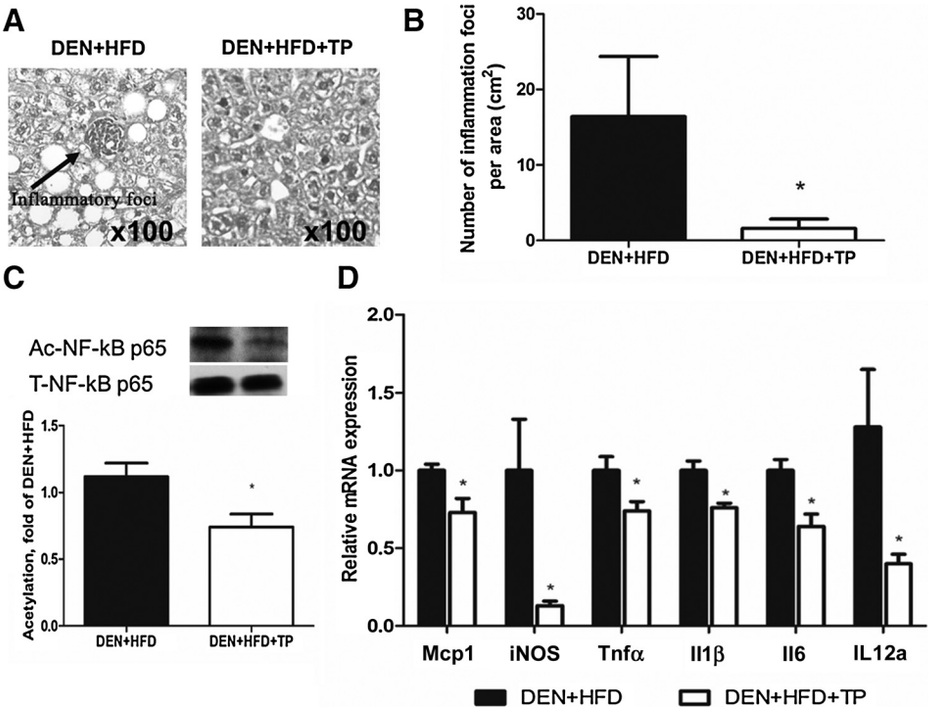

Figure 4.
Effects of TP feeding on inflammation foci and hepatic mRNA and protein expression of Ac-NF-κB and its downstream genes in DEN+HFD-fed $BCO1^{-/-}BCO2^{-/-}$ double KO mice. **A,** The histopathologic images of inflammation foci between DEN+HFD and DEN+HFD+TP groups. **B,** The difference in inflammation foci numbers between DEN+HFD and DEN+HFD+TP groups. Graphical representation of fold change in (**C**) Ac-NF-κB protein and (**D**) MCP1, iNOS, TNFα, IL1β, IL6, and IL12 α genes. Values are expressed as mean ± SEM. Differences between groups were analyzed by Student *t* test. *Significantly different from the DEN+HFD, $P < 0.05$.

Parabacteroides, *Escherichia*, and *Bifidobacterium* were the most predominant. *Bacteroides* and *Parabacteroides* were members of the phylum *Bacteroidetes*, *Clostridium* and *Lactobacillus* belonged to the phylum *Firmicutes*, *Mucispirillum* was classified as the phylum *Deferribacteres*, *Escherichia* and *Bifidobacterium* were in the phylum *Proteobacteria* and *Actiobacteria*, respectively. Relative abundance of *Bacteroides*, *Mucispirillum*, *Clostridium*, and *Parabacteroides* decreased, and *Lactobacillus* and *Bifidobacterium* increased in the TP supplementation group (Fig. 5E). At the species level, 34 species were detected between the DEN+HFD and DEN+HFD+TP groups (Fig. 5F). Of 9 prominent species, 6 were *Firmicutes*. The remaining 3 belonged to *Bacteroidetes*, *Deferribacteres*, and *Proteobacterias*, respectively. The relative abundance of phylum *Deferribacteres* (Fig. 6A) and its correspondent genus *Mucispirillum* (Fig. 6B) and species *Mucispirillum schaedleri* (Fig. 6C) decreased significantly when comparing the HFD+DEN and HFD+DEN+TP groups. Furthermore, TP supplementation significantly decreased the relative abundance of genus *Clostridium* ($P = 0.05$; Fig. 6D). The relative abundance of species *Clostridium sp. Clone-9* (Fig. 6E) increased, and species *Clostridium sp.ID4* (Fig. 6F) decreased significantly.

Discussion

This is the first study to provide evidence that TP feeding (tomato as a whole food) has beneficial effects against DEN-initiated, HFD-promoted HCC incidence and multiplicity. Despite that genetic variation of BCO1 and BCO2 can affect the metabolism of a variety of carotenoids, including lycopene, which has been shown in humans (32), in the present study, TP feeding inhibited the multiplicity and volume of HCC and attenuated steatosis severity in $BCO1^{-/-}BCO2^{-/-}$ double KO mice. This indicates that lycopene-rich tomato and tomato products can play a positive role in their own antitumor activity in the absence of BCO1 or/and BCO2 enzymes. Although we previously demonstrated that the chemopreventive effect of lycopene in BCO2 single KO mice was similar to that of wild-type mice and lycopene feeding (100 mg/kg diet) for 24 weeks resulted in suppressing both incidence (19%) and multiplicity (58%) of HCC in mice (15), in the present study, we observed that TP feeding (equivalent to lycopene 100 mg/kg diet as previously used) is more effective than the same dose of purified lycopene (14) to inhibit HCC development [e.g., resulted in suppressing HCC incidence (67%) and multiplicity (83%) and tumor volume (95%) for 24 weeks]. This was consistent with our previous study that the lycopene supplement was effective in inhibiting DEN-initiated HCC in the BCO2 KO mice (14). The present study provides an idea of the population-based or clinical trial effects of tomato and tomato products or lycopene on liver cancer prevention in humans with the existence of a BCO1/BCO2 polymorphism in the future.

SIRT1 is a NAD-dependent protein deacetylase, which catalyzes the deacetylation of many histones and nonhistone proteins including NF-κB, FOXOs (forkhead transcription factors), p53, and more (31). By deacetylating

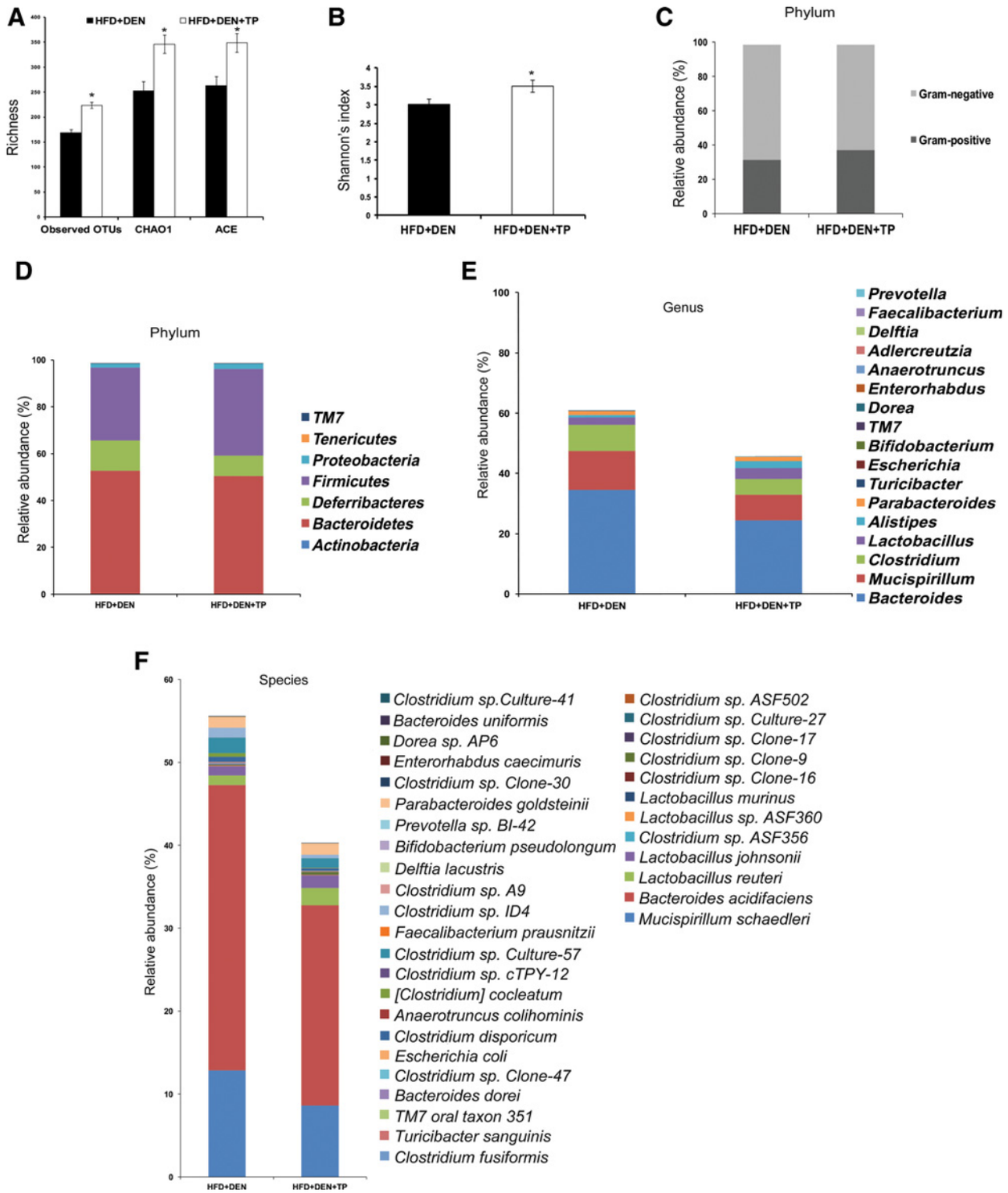

Figure 5.

Effects of TP feeding on microbiota richness and distribution at phylum, genus, and species levels in DEN+HFD-fed $BCO1^{-/-}BCO2^{-/-}$ double KO mice. **A,** Observed OTUs, Chao1, and ACE, representing community richness. **B,** Shannon index, representing community evenness. **C,** Relative abundance of gram-positive bacteria or gram-negative bacteria. **D,** Relative abundance of major bacteria at phylum level. **E** and **F,** Relative abundance of major bacteria at genus, species levels. *Significantly different from the DEN+HFD, $P < 0.05$.

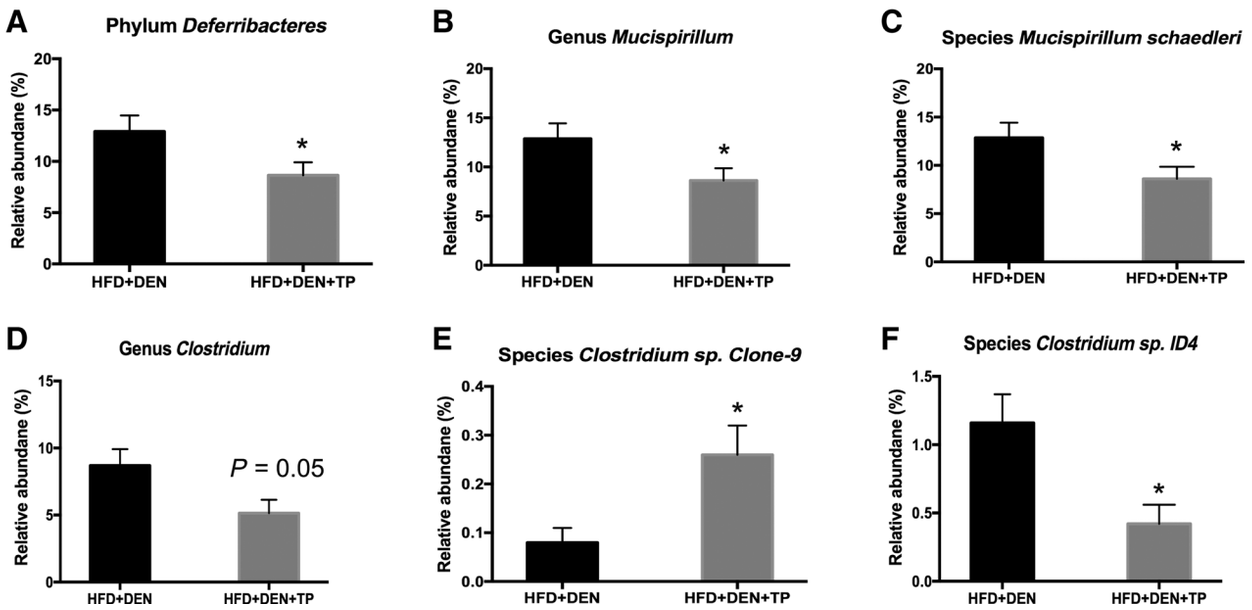

Figure 6.

Effects of TP feeding on *Mucispirillum* and *Clostridium* abundance in DEN+HFD-fed BCO1$^{-/-}$BCO2$^{-/-}$ double KO mice. **A,** *Deferribacteres* abundance at phylum level between DEN+HFD and DEN+HFD+TP groups. **B** and **C,** Relative abundance of genus *Mucispirillum* and species *Mucispirillum schaedleri* as part of phylum *Deferribacteres*. **D,** Relative abundance of *Clostridium* at genus level. **E,** and **F,** Relative abundance of *Clostridium sp.ID4* and *Clostridium sp.Clone.9* at species level. *Significantly different from the DEN+HFD, $P < 0.05$.

transcription factors and cofactors, SIRT1 plays a beneficial role in regulating hepatic lipid metabolism, liver steatosis, and tumorigenesis (33). We have reported that ablation of SIRT1 caused an overloaded accumulation of hepatic triglyceride with higher levels of SREBP-1 and SCD1 and lower levels of phosphorylation of LKB1 and AMPK in the liver, and higher mRNA expression of lipogenic genes in the mesenteric adipose tissue (34). In the present study, TP feeding increased the expression mRNA and protein levels of SIRT1 and decreased acetylation of FOXO1 significantly without changing the total FOXO1 level in DEN+HFD and BCO1$^{-/-}$BCO2$^{-/-}$ double KO mice, which indicated an increased deacetylase activity of SIRT1 and may explain the reduction of tumor incidence. NAMPT catalyzes the rate-limiting step of NAD^+ synthesis and directly regulates the expression of SIRT1 (35). We found that NAMPT increased after TP feeding in the liver tissues of DEN+HFD, BCO1$^{-/-}$BCO2$^{-/-}$ double KO mice, which may account for the enhanced deacetylation activity of SIRT1. AMPK is considered a critical sensor of energy metabolism (36) and plays a role in linking metabolic disease and cancer (37) by regulating cell cycle, cell polarity, senescence, autophagy, and apoptosis in cancer progression (38). In our study, we found phosphorylated AMPK was increased by TP feeding, which indicates TP feeding may activate AMPK and further influence lipid metabolism and HCC development. Combined with upregulation of SIRT1 in the present study, evidence showed that AMPK enhances the activity of the gene expression in coordination with SIRT1, which may explain the convergent biological effects of AMPK and SIRT1 on energy metabolism and tumor progression (39). We further investigated the downstream mRNA expressions of AMPK. We found that TP feeding increased PPARα, PGC-1α, ACOX1, and CPT1 expressions in hepatic tissues, which mainly upregulate fatty acid β-oxidation in mitochondria and decrease lipid accumulation (40). In addition, activated PPARα can further enhance the transcription of ACOX1 and CPT1 (41). TP feeding decreased CD36 levels, which can be induced by AMPK and regulate fatty acid uptake (42). In addition, TP feeding reduced synthesis of triacylglycerol and inhibited the cancer cell growth by downregulating DGAT1 (43). Above all, TP feeding regulates lipid metabolism of HCC development through the SIRT1/AMPK pathway by reducing fatty acid accumulation and synthesis of triacylglycerol, and upregulation of fatty acid uptake.

The circadian clock system maintains biological rhythmic function consisting of two components: a central clock in the brain and a peripheral clock in all body tissues. Peripheral clock genes in the liver play fundamental roles in maintaining liver homeostasis (44). Circadian disorder can increase carcinogenesis and fasten tumor growth (45). The present study is the first study to show that TP feeding increases Clock gene expression significantly in DEN+HFD and BCO1$^{-/-}$BCO2$^{-/-}$ double KO mice. In addition to regulating hepatic lipid metabolism, steatosis, and tumorigenesis, SIRT1 interacts with

Clock and Bmal1 and then upregulates the expression of NAMPT by binding to E-box elements (44). Because SIRT1 uses NAD^+ as a coenzyme to deacetylate circadian clock proteins, including Bmal1 and Per2, and regulates PCG-1α, FOXO1 (44), which indicates that TP feeding may regulate DEN+HFD-induced hepatic lesions and HCC development through the SIRT1/Clock pathway. The core circadian transcription factor Clock and Bmal1 can regulate the transcription of clock-controlled genes followed by activation of Per and Cry (46). Mutant Per2 mice exhibited increased tumorigenesis compared with wild-type mice, which may be related to a deficiency in p53, a cancer-suppressor gene (47). As the key clock genes, evidence showed that Cry2 rhythm in the fibrotic livers was impaired compared with normal livers (48). In our study, the Cry2 level was more significantly increased after TP feeding than the group without TP intervention. We also observed that the TP feeding increased the level of Wee1 expression in the liver. Wee1, a protein kinase, regulates the cell cycle by controlling cell entry into mitosis at the G_2–M checkpoint through activation of cyclin-dependent kinase 1 (CDK1), inactivates G_2 arrest, and repairs DNA damage resulting in cancer cell death (49). Together, the regulation of these key circadian clock genes including Clock, Per2, Cry2, and Wee1 could contribute to chemopreventive effects of TP feeding against HFD-promoted HCC development.

In tumor-related inflammation key factors, NF-κB has a prominent role (50). The wide variety of genes regulated by NF-κB includes encoding cytokines (e.g., IL1, IL2, IL6, IL12, TNFα), chemokines (e.g., MCP1, IL8), and inducible effector enzymes (e.g., iNOS, COX-2; ref. 51). In our study, the TP feeding significantly decreased HFD-induced hepatic inflammatory foci and acetylation-NF-κB p65, which indicated the role that tomato as a whole food plays in inhibiting the HFD-promoted HCC by inhibiting inflammation. We also observed that mRNA expression levels of Mcp1, iNOS, TNFα, IL1β, IL6, and IL12α decreased significantly in the DEN+HFD+TP feeding group, compared with the DEN+HFD group. Since inflammation cell infiltration, one of the main characteristics for NASH, is a more aggressive form with necroinflammation, fibrosis, and promoting HCC development. The downregulation of NF-κB by TP feeding exhibits the potential mechanism in anti-inflammation/anticarcinogenesis activity of tomato and tomato products consumption.

Liver is the most related to the intestinal tract by defending detrimental bacterial composition and metabolites through portal circulation (52). Decreased fecal gut microbial richness was found in those NASH patients compared with controls (7), which is a risk factor of HCC, a long-term consequence of aforementioned chronic liver injury, inflammation, and fibrosis (2). In our present study, TP feeding significantly increased the richness and diversity of gut microbiota in the DEN+HFD group. Recently, new evidence showed that the gut microbiome also displayed a circadian rhythm pattern by impairing the hepatic circadian clock gene expression and specific bacterial metabolites in the microbial depletion germ-free (52). Gut microbiota contains gram-positive and gram-negative bacteria; overgrowth of gram-negative bacteria can increase the production of hepatotoxic products such as lipopolysaccharide (LPS; ref. 53). In the present study, a reduced tendency of relative abundance of gram-negative bacteria indicated that TP feeding may reduce the production of LPS, which induces inflammation by activating Toll-like receptors 4, promoting cell proliferation, and cell apoptosis resistance (54). We found 3 main phylums in this study and only phylum *Deferribacteres* and its corresponding genus and species, as well as a relative abundance of *Mucispirillum* and *Mucispirillum schaedleri*, which significantly decreased after TP feeding. *Mucispirillum* has been associated with inflammation markers and increased serum leptin levels (55), which suggested that TP feeding may decrease the inflamed cytokines through reduction of gut microbiota of *Mucispirillum* as well. The total change of genus *Clostridium* was decreased after TP supplementation ($P = 0.05$). In addition, as a part of genus *Clostridium*, *Clostridium sp.ID4* decreased significantly in the TP feeding group, and *Clostridium sp.Clone.9* increased significantly in the TP feeding group. Evidence indicated that increased *Clostridium* is involved in increased hepatic lipogenesis and reduced fatty acid oxidation (56). However, the biological properties of species *Clostridium sp.ID4* and *Clostridium sp.Clone.9* have not been characterized yet. In our previous study of TP feeding against NAFLD, relative abundance of species *Clostridium sp. ID4* decreased as well (27), which indicated that *Clostridium sp. ID4* may be a potential target of TP feeding. Together, TP feeding increased the richness and diversity of gut microbiome and improved some beneficial bacteria, which in turns helps regulating hepatic inflammation, hepatic lipid metabolism, and hepatic circadian clock by gut–liver interaction.

One of our limitations is that the main content of TP is lycopene, but we cannot determine the potential beneficial effects of other nutrients in a whole tomato, such as apolycopenoids, vitamin E, vitamin C, β-carotene, minerals, phenolic compounds, and dietary fibers. For example, we cannot exclude the possibility that TP inhibits HCC development in the BCO1/BCO2 double KO mice due to apo-lycopenoids produced by other unidentified cleavage enzymes (e.g., carotenoid cleavage enzymes do exist in both bacteria and plants, including tomatoes). In plants, the production of apocarotenoids from carotenoids is catalyzed by a family of carotenoid cleavage dioxygenases which cleave the 9′,10′double bonds of carotenoids including lycopene (57). A series of apolycopenoids, including apo-10′-

lycopenal, have been identified in human plasmas of humans who consumed tomato juice for 8 weeks (4 to 8 ounces delivering 21.9 mg of lycopene/day; ref. 58). Although we did not detect any apo-lycopenoids in the livers of the animal in the present study, we believe that the chemopreventive actions of consumption of lycopene-rich whole foods may be more efficacious than isolated lycopene by targeting multiple molecular and cellular pathways.

Disclosure of Potential Conflicts of Interest

No potential conflicts of interest were disclosed.

Disclaimer

Any opinions, findings, conclusions, and recommendations expressed in this publication are those of the author(s) and do not necessarily reflect the views of the sponsors.

Authors' Contributions

Conception and design: K. Aizawa, X.-D. Wang
Development of methodology: H. Xia, C. Liu, K.-Q. Hu
Acquisition of data (provided animals, acquired and managed patients, provided facilities, etc.): H. Xia, C. Liu, S. Takahashi
Analysis and interpretation of data (e.g., statistical analysis, biostatistics, computational analysis): H. Xia, C. Liu, C.-C. Li, M. Fu, S. Takahashi, K. Aizawa, L. Zhao, X.-D. Wang
Writing, review, and/or revision of the manuscript: H. Xia, C. Liu, S. Hiroyuki, G. Wu, L. Zhao, X.-D. Wang
Administrative, technical, or material support (i.e., reporting or organizing data, constructing databases): C. Liu
Study supervision: S. Hiroyuki, X.-D. Wang

Acknowledgments

We thank Jenna M. Sills and Dr. Donald E. Smith for their assistance. H. Xia is supported by a scholarship from Key Laboratory of Environmental Medicine and Engineering of Ministry of Education and Department of Nutrition and Food Hygiene, School of Public Health, Southeast University, Nanjing, P.R. China.

This study was supported by the US Department of Agriculture NIFA/AFRI grants 2015-67017-23141 (to X.-D. Wang) and USDA/ARS 1950-51000-074S (to X.-D. Wang).

The costs of publication of this article were defrayed in part by the payment of page charges. This article must therefore be hereby marked *advertisement* in accordance with 18 U.S.C. Section 1734 solely to indicate this fact.

Received May 29, 2018; revised August 28, 2018; accepted October 2, 2018; published first November 16, 2018.

References

1. Wong RJ, Cheung R, Ahmed A. Nonalcoholic steatohepatitis is the most rapidly growing indication for liver transplantation in patients with hepatocellular carcinoma in the U.S. Hepatology 2014;59:2188–95.
2. White DL, Kanwal F, El-Serag HB. Association between nonalcoholic fatty liver disease and risk for hepatocellular cancer, based on systematic review. Clin Gastroenterol Hepatol 2012;10:1342–59.e2.
3. Siegel RL, Miller KD, Jemal A. Cancer statistics, 2016. CA Cancer J Clin 2016;66:7–30.
4. Valery PC, Laversanne M, Clark PJ, Petrick JL, McGlynn KA, Bray F. Projections of primary liver cancer to 2030 in 30 countries worldwide. Hepatology 2018;67:600–11.
5. Saltzman ET, Palacios T, Thomsen M, Vitetta L. Intestinal microbiome shifts, dysbiosis, inflammation, and non-alcoholic fatty liver disease. Front Microbiol 2018;9:61.
6. Cani PD, Bibiloni R, Knauf C, Waget A, Neyrinck AM, Delzenne NM, et al. Changes in gut microbiota control metabolic endotoxemia-induced inflammation in high-fat diet-induced obesity and diabetes in mice. Diabetes 2008;57:1470–81.
7. Zhu L, Baker SS, Gill C, Liu W, Alkhouri R, Baker RD, et al. Characterization of gut microbiomes in nonalcoholic steatohepatitis (NASH) patients: a connection between endogenous alcohol and NASH. Hepatology 2013;57:601–9.
8. Yoshimoto S, Loo TM, Atarashi K, Kanda H, Sato S, Oyadomari S, et al. Obesity-induced gut microbial metabolite promotes liver cancer through senescence secretome. Nature 2013;499:97–101.
9. Said A, Ghufran A. Epidemic of non-alcoholic fatty liver disease and hepatocellular carcinoma. World J Clin Oncol 2017;8:429–36.
10. Clinton SK. Lycopene: chemistry, biology, and implications for human health and disease. Nutr Rev 1998;56(2 Pt 1):35–51.
11. Giovannucci E. Tomatoes, tomato-based products, lycopene, and cancer: review of the epidemiologic literature. J Natl Cancer Inst 1999;91:317–31.
12. Mein JR, Lian F, Wang XD. Biological activity of lycopene metabolites: implications for cancer prevention. Nutr Rev 2008;66:667–83.
13. Ip BC, Wang XD. Non-alcoholic steatohepatitis and hepatocellular carcinoma: implications for lycopene intervention. Nutrients 2014;6:124–62.
14. Ip BC, Liu C, Ausman LM, von Lintig J, Wang XD. Lycopene attenuated hepatic tumorigenesis via differential mechanisms depending on carotenoid cleavage enzyme in mice. Cancer Prev Res (Phila) 2014;7:1219–27.
15. Ip BC, Hu KQ, Liu C, Smith DE, Obin MS, Ausman LM, et al. Lycopene metabolite, apo-10′-lycopenoic acid, inhibits diethylnitrosamine-initiated, high fat diet-promoted hepatic inflammation and tumorigenesis in mice. Cancer Prev Res (Phila) 2013;6:1304–16.
16. Hu KQ, Liu C, Ernst H, Krinsky NI, Russell RM, Wang XD. The biochemical characterization of ferret carotene-9′,10′-monooxygenase catalyzing cleavage of carotenoids in vitro and in vivo. J Biol Chem 2006;281:19327–38.
17. Tan HL, Moran NE, Cichon MJ, Riedl KM, Schwartz SJ, Erdman JW Jr, et al. Beta-Carotene-9′,10′-oxygenase status modulates the impact of dietary tomato and lycopene on hepatic nuclear receptor-, stress-, and metabolism-related gene expression in mice. J Nutr 2014;144:431–9.
18. Dela Sena C, Narayanasamy S, Riedl KM, Curley RW Jr, Schwartz SJ, Harrison EH. Substrate specificity of purified recombinant human beta-carotene 15,15′-oxygenase (BCO1). J Biol Chem 2013;288:37094–103.

19. Von Lintig J. Colors with functions: elucidating the biochemical and molecular basis of carotenoid metabolism. Annu Rev Nutr 2010;30:35–56.
20. Wang XD. Lycopene metabolism and its biological significance. Am J Clin Nutr 2012;96:1214s–22s.
21. Lietz G, Oxley A, Boesch-Saadatmandi C, Kobayashi D. Importance of beta,beta-carotene 15,15′-monooxygenase 1 (BCMO1) and beta,beta-carotene 9′,10′-dioxygenase 2 (BCDO2) in nutrition and health. Mol Nutr Food Res 2012;56:241–50.
22. Ferrucci L, Perry JR, Matteini A, Perola M, Tanaka T, Silander K, et al. Common variation in the beta-carotene 15,15′-monooxygenase 1 gene affects circulating levels of carotenoids: a genome-wide association study. Am J Hum Genet 2009;84:123–33.
23. Borel P. Genetic variations involved in interindividual variability in carotenoid status. Mol Nutr Food Res 2012;56:228–40.
24. Ford NA, Clinton SK, von Lintig J, Wyss A, Erdman JW Jr. Loss of carotene-9′,10′-monooxygenase expression increases serum and tissue lycopene concentrations in lycopene-fed mice. J Nutr 2010;140:2134–8.
25. Tian R, Pitchford WS, Morris CA, Cullen NG, Bottema CD. Genetic variation in the beta, beta-carotene-9′, 10′-dioxygenase gene and association with fat colour in bovine adipose tissue and milk. Anim Genet 2010;41:253–9.
26. Lim JY, Liu C, Hu K-Q, Smith DE, Wang XD. Ablation of carotenoid cleavage enzymes (BCO1 and BCO2) induced hepatic steatosis by altering the farnesoid X receptor/miR-34a/sirtuin 1 pathway. Arch Biochem Biophys 2018;654:1–9.
27. Li CC, Liu C, Fu M, Hu KQ, Aizawa K, Takahashi S, et al. Tomato powder inhibits hepatic steatosis and inflammation potentially through restoring SIRT1 activity and adiponectin function independent of carotenoid cleavage enzymes in mice. Mol Nutr Food Res 2018;62:e1700738.
28. Palczewski G, Widjaja-Adhi MA, Amengual J, Golczak M, von Lintig J. Genetic dissection in a mouse model reveals interactions between carotenoids and lipid metabolism. J Lipid Res 2016;57:1684–95.
29. Kim SW, Suda W, Kim S, Oshima K, Fukuda S, Ohno H, et al. Robustness of gut microbiota of healthy adults in response to probiotic intervention revealed by high-throughput pyrosequencing. DNA Res 2013;20:241–53.
30. Schmitz HH, Poor CL, Wellman RB, Erdman JW Jr. Concentrations of selected carotenoids and vitamin A in human liver, kidney and lung tissue. J Nutr 1991;121:1613–21.
31. Baur JA, Ungvari Z, Minor RK, Le Couteur DG, de Cabo R. Are sirtuins viable targets for improving healthspan and lifespan? Nat Rev Drug Discov 2012;11:443–61.
32. Lietz G, Oxley A, Leung W, Hesketh J. Single nucleotide polymorphisms upstream from the beta-carotene 15,15′-monoxygenase gene influence provitamin A conversion efficiency in female volunteers. J Nutr 2012;142:161s–5s.
33. Herranz D, Serrano M. SIRT1: recent lessons from mouse models. Nat Rev Cancer 2010;10:819–23.
34. Cheng J, Liu C, Hu K, Greenberg A, Wu D, Ausman LM, et al. Ablation of systemic SIRT1 activity promotes nonalcoholic fatty liver disease by affecting liver-mesenteric adipose tissue fatty acid mobilization. Biochim Biophys Acta 2017;1863:2783–90.
35. Shackelford RE, Mayhall K, Maxwell NM, Kandil E, Coppola D. Nicotinamide phosphoribosyltransferase in malignancy: a review. Genes Cancer 2013;4:447–56.
36. Zong H, Ren JM, Young LH, Pypaert M, Mu J, Birnbaum MJ, et al. AMP kinase is required for mitochondrial biogenesis in skeletal muscle in response to chronic energy deprivation. Proc Natl Acad Sci U S A 2002;99:15983–7.
37. Luo Z, Zang M, Guo W. AMPK as a metabolic tumor suppressor: control of metabolism and cell growth. Future Oncol 2010;6:457–70.
38. Wang W, Guan KL. AMP-activated protein kinase and cancer. Acta Physiol (Oxf) 2009;196:55–63.
39. Canto C, Gerhart-Hines Z, Feige JN, Lagouge M, Noriega L, Milne JC, et al. AMPK regulates energy expenditure by modulating NAD+ metabolism and SIRT1 activity. Nature 2009;458:1056–60.
40. Cohen JC, Horton JD, Hobbs HH. Human fatty liver disease: old questions and new insights. Science 2011;332:1519–23.
41. Chitturi S, Abeygunasekera S, Farrell GC, Holmes-Walker J, Hui JM, Fung C, et al. NASH and insulin resistance: insulin hypersecretion and specific association with the insulin resistance syndrome. Hepatology 2002;35:373–9.
42. Choi YJ, Lee KY, Jung SH, Kim HS, Shim G, Kim MG, et al. Activation of AMPK by berberine induces hepatic lipid accumulation by upregulation of fatty acid translocase CD36 in mice. Toxicol Appl Pharmacol 2017;316:74–82.
43. Mitra R, Le TT, Gorjala P, Goodman OB Jr. Positive regulation of prostate cancer cell growth by lipid droplet forming and processing enzymes DGAT1 and ABHD5. BMC Cancer 2017;17:631.
44. Tahara Y, Shibata S. Circadian rhythms of liver physiology and disease: experimental and clinical evidence. Nat Rev Gastroenterol Hepatol 2016;13:217–26.
45. Kiessling S, Cermakian N. The tumor circadian clock: a new target for cancer therapy? Future Oncol 2017;13:2607–10.
46. Gaucher J, Montellier E, Sassone-Corsi P. Molecular cogs: interplay between circadian clock and cell cycle. Trends Cell Biol 2018;28:368–79.
47. Fu L, Pelicano H, Liu J, Huang P, Lee C. The circadian gene Period2 plays an important role in tumor suppression and DNA damage response in vivo. Cell 2002;111:41–50.
48. Chen P, Kakan X, Zhang J. Altered circadian rhythm of the clock genes in fibrotic livers induced by carbon tetrachloride. FEBS Lett 2010;584:1597–601.
49. Webster PJ, Littlejohns AT, Gaunt HJ, Young RS, Rode B, Ritchie JE, et al. Upregulated WEE1 protects endothelial cells of colorectal cancer liver metastases. Oncotarget 2017;8:42288–99.
50. Berasain C, Castillo J, Perugorria MJ, Latasa MU, Prieto J, Avila MA. Inflammation and liver cancer: new molecular links. Ann N Y Acad Sci 2009;1155:206–21.
51. Ghosh S, Karin M. Missing pieces in the NF-kappaB puzzle. Cell 2002;109 Suppl:S81–96.
52. Fu ZD, Cui JY. Remote sensing between liver and intestine: importance of microbial metabolites. Curr Pharmacol Rep 2017;3:101–13.
53. Wigg AJ, Roberts-Thomson IC, Dymock RB, McCarthy PJ, Grose RH, Cummins AG. The role of small intestinal bacterial overgrowth, intestinal permeability, endotoxaemia, and tumour necrosis factor alpha in the pathogenesis of non-alcoholic steatohepatitis. Gut 2001;48:206–11.
54. Gu J, Sun R, Shen S, Yu Z. The influence of TLR4 agonist lipopolysaccharides on hepatocellular carcinoma cells and the feasibility of its application in treating liver cancer. Onco Targets Ther 2015;8:2215–25.
55. Loy A, Pfann C, Steinberger M, Hanson B, Herp S, Brugiroux S, et al. Lifestyle and horizontal gene transfer-mediated evolution

of mucispirillum schaedleri, a core member of the murine gut microbiota. mSystems 2017;2.
56. Mokhtari Z, Gibson DL, Hekmatdoost A. Nonalcoholic fatty liver disease, the gut microbiome, and diet. Adv Nutr 2017;8: 240–52.
57. Vogel JT, Tan BC, McCarty DR, Klee HJ. The carotenoid cleavage dioxygenase 1 enzyme has broad substrate specificity, cleaving multiple carotenoids at two different bond positions. J Biol Chem 2008;283:11364–73.
58. Kopec RE, Riedl KM, Harrison EH, Curley RW Jr, Hruszkewycz DP, Clinton SK, et al. Identification and quantification of apo-lycopenals in fruits, vegetables, and human plasma. J Agric Food Chem 2010;58: 3290–6.